

Trade-Offs between Speed, Accuracy, and Dissipation in tRNA^{Ile} Aminoacylation

Qiwei Yu, Joel D. Mallory, Anatoly B. Kolomeisky, Jiqiang Ling, and Oleg A. Igoshin*

Cite This: *J. Phys. Chem. Lett.* 2020, 11, 4001–4007

Read Online

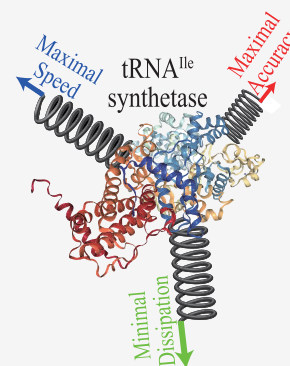
ACCESS |

Metrics & More

Article Recommendations

Supporting Information

ABSTRACT: Living systems maintain a high fidelity in information processing through kinetic proofreading, a mechanism for preferentially removing incorrect substrates at the cost of energy dissipation and slower speed. Proofreading mechanisms must balance their demand for higher speed, fewer errors, and lower dissipation, but it is unclear how rates of individual reaction steps are evolutionarily tuned to balance these needs, especially when multiple proofreading mechanisms are present. Here, using a discrete-state stochastic model, we analyze the optimization strategies in *Escherichia coli* isoleucyl-tRNA synthetase. Surprisingly, this enzyme adopts an economic proofreading strategy and improves speed and dissipation as long as the error is tolerable. Through global parameter sampling, we reveal a fundamental dissipation–error relation that bounds the enzyme’s optimal performance and explains the importance of the post-transfer editing mechanism. The proximity of native system parameters to this bound demonstrates the importance of energy dissipation as an evolutionary force affecting fitness.



The fitness of many organisms relies on the fidelity and reliability of information propagation, epitomized by remarkable accuracy in DNA replication, mRNA transcription, and protein translation.^{1–5} It is well-known that many biological systems adopt kinetic proofreading (KPR), a mechanism that actively removes wrongly incorporated substrates, to reduce the error beyond the equilibrium limit.^{6,7} The KPR mechanism is not only vital to cell viability^{8,9} but also of great interest in the field of nonequilibrium thermodynamics.^{10–13}

Ideally, biological systems should process information rapidly while keeping error and dissipation low. Theoretical studies, nonetheless, have revealed that it is impossible to optimize the three properties (speed, error, and dissipation) simultaneously.^{14,15} For example, the accuracy of copying a single bit of information is highest in either a slow and quasi-adiabatic regime or a fast and dissipative one, demonstrating a trade-off between speed and dissipation.¹¹ Similar trade-offs involving the error also exist.¹³ Resolving these trade-offs requires biological systems to prioritize different properties. For replication and translation, enzymes were shown to optimize speed over error and dissipation.^{14,16} It is, however, unclear whether the same preference applies to more complex proofreading systems. For example, many enzymes exhibit multistage proofreading; i.e., the enzyme–substrate complex can undergo proofreading and be reset to the initial state at more than one state. Previous studies of multistage proofreading have focused on systems with discrimination between cognate and noncognate substrates only in dissociation steps.^{10,12} However, experimental evidence suggests that the discrimination can occur in any step.^{4,5,17–20} Thus, a

systematic investigation of the speed–accuracy–dissipation relation in a biologically relevant context is still lacking.

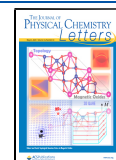
Isoleucyl-tRNA synthetase (IleRS) in *Escherichia coli* is one of the best characterized multistage proofreading systems. During protein synthesis, IleRS must accurately pair cognate tRNA^{Ile} with the corresponding amino acid, i.e., isoleucine.²¹ Misincorporation has severe physiological impacts, including increasing the DNA mutation rate.²² IleRS utilizes multiple proofreading pathways to remove noncognate valine, an amino acid chemically similar to isoleucine. The proofreading mechanisms can be divided into pre-transfer editing, which occurs within the active (synthetic) site, and post-transfer editing, which occurs at a separate editing site.^{21,23} In this work, we construct a biologically relevant model of IleRS (see Figure 1) and extract parameters from experimental data to address three questions: (i) how the rates of individual reaction steps are optimized to deal with the speed–error–dissipation trade-off, (ii) whether there is a fundamental limit on the extent of overall optimization and, if so, where *E. coli* IleRS is relative to that limit, and (iii) whether there is an evolutionary reason for the existence of multiple proofreading pathways.

To this end, we quantitatively study the IleRS network using a discrete-state stochastic framework previously employed in

Received: April 6, 2020

Accepted: April 30, 2020

Published: April 30, 2020



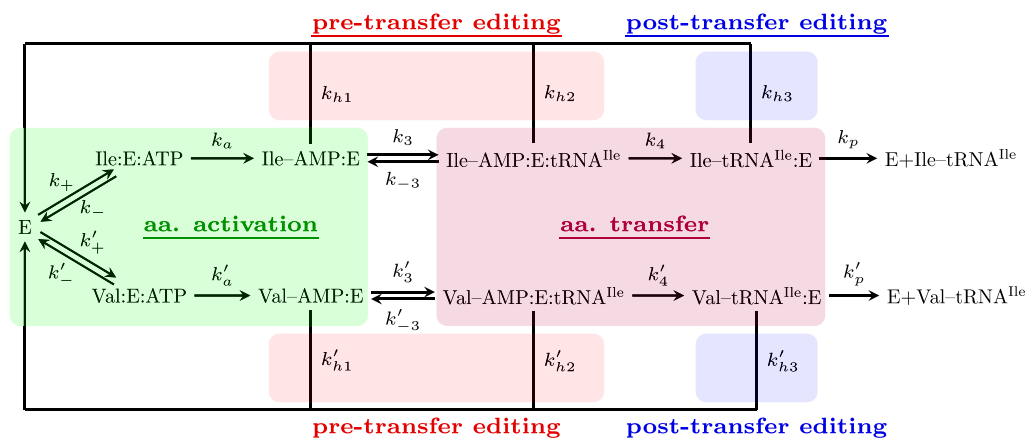


Figure 1. Chemical reaction network for the aminoacylation of tRNA^{Ile} in *E. coli*. Abbreviations: E, isoleucyl-tRNA synthetase (IleRS); Ile, isoleucine; Val, valine. The rate constants are labeled k_i for the right pathway (isoleucine pathway) and k'_i for the wrong pathway (valine pathway). The three proofreading pathways are labeled as k_{h1} , k_{h2} , k_{h3} , and their primed counterparts. Although the reverse reactions are not drawn for some reactions that are kinetically driven forward, they are technically all reversible. We include them in the simulation to maintain thermodynamic consistency.

the study of T7 DNA polymerase and *E. coli* ribosome.^{14,16} The chemical steps in Figure 1 are modeled as quasi-first-order transitions between different states with rates estimated from quantitative kinetic experiments^{5,19,24–37} (see the Supporting Information for details). We define the error (η) as the ratio of the splitting probability of forming an incorrect product to the splitting probability of forming a correct product. The speed is quantified by the inverse of the conditional mean first-passage time (MFPT, τ) to form a correct product starting from the free enzyme state (E). The dissipation is defined as the amount of free energy dissipated per product formed (σ , in units of $k_B T$).³⁸ The detailed mathematical definitions and procedures can be found in the Supporting Information.

Due to the symmetry of the reaction network, each process for the noncognate amino acid (with rate k'_i) has a corresponding reaction in the cognate reaction network (with rate k_i). We relate those two reactions by defining a set of discrimination factors $f_i = k'_i/k_i$, where i is a subscript unique to individual reactions. The discrimination factors are the fundamental factor that differentiates the cognate reactant from the noncognate one. We study the interplay between three characteristic properties (speed, error, and dissipation) by proportionally varying the rate constants (k_i and k'_i) while keeping the discrimination factors f_i fixed. In this way, neither of the substrates receives any unfair advantage. A trade-off between two properties occurs if a change in a given rate constant cannot simultaneously improve both of them. Thus, the trade-offs among speed, error, and dissipation must be discussed in the context of a specific set of rate constant perturbations. We investigate the effect of tuning either one rate constant (local parameter perturbation) or tuning multiple rate constants (global parameter perturbation).

We begin our analysis with two catalytic steps: amino acid activation and transfer, denoted by k_a and k_4 , respectively (see Figure 1). These two processes are energetically important because they involve covalent bond breakage and formation, thereby channeling the energy stored in the phosphoanhydride bonds of ATP to that in the ester bond of aa-tRNA. The energy transferred provides the driving force for subsequent peptide bond synthesis in the ribosome. To uncover the optimization for these steps, we analyze how the characteristic

properties change as a function of their respective rate constants (k_a and k_4).

The results shown in Figure 2 are somewhat unexpected. First, both speed and accuracy can be improved simultaneously

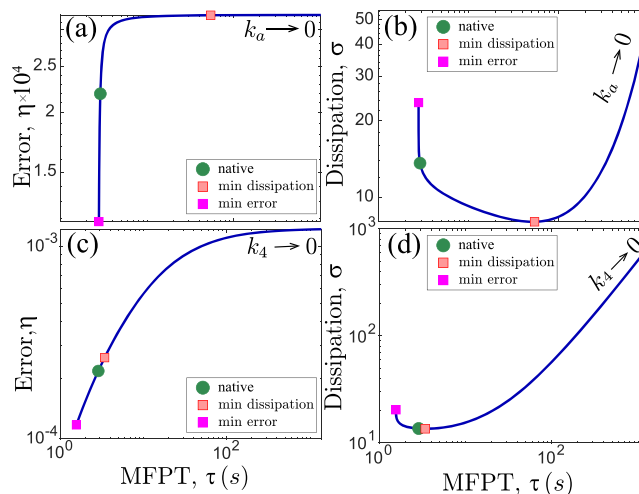


Figure 2. Trade-off among MFPT (τ), error (η), and dissipation (σ) due to variation of the two key catalytic steps: amino acid activation coupled to ATP hydrolysis (k_a , top panels) and amino acid transfer (k_4 , bottom panels). Catalytic rates for the noncognate substrates (k'_a and k'_4) are varied proportionally to keep the discrimination factors fixed. The green dot denotes the native system. The pink and magenta squares correspond to the positions of the minimum dissipation and error, respectively. The termination of the curve at the magenta squares is not a result of an insufficient sampling range but a limit that cannot be passed even when the rates go to infinity.

by increasing the catalytic rates of both reactions: this result demonstrates a lack of trade-off between the two properties (Figure 2a,c). Indeed, the synthetase has a higher affinity for isoleucine than for valine, which results in catalytic rates slightly higher than that of valine. In other words, the discrimination factors f_a and f_4 are slightly smaller than 1.¹⁹ Therefore, accelerating these steps magnifies the discrimination in these two steps and results in higher speed and accuracy for IleRS. Second, the relation between speed and

dissipation is nonmonotonic (Figure 2b,d). Consequently, the MFPT–dissipation curve can be separated into two branches: a trade-off branch where reducing dissipation inevitably increases MFPT and a non-trade-off branch where the two properties can be improved simultaneously. However, for both steps, the native system (i.e., the green dot corresponding to experimentally measured rates of these steps) resides on the trade-off branch. The fact that the native system also resides between the minima of error and dissipation (magenta and pink squares) indicates a trade-off between these two properties, as well. Therefore, it is the dissipation that prevents the co-optimization of speed and accuracy. This result is analogous to prior findings for the Pol-Exo sliding in T7 DNA polymerase and the proofreading rate in aa-tRNA selection by *E. coli* ribosome.¹⁴

Qualitatively, the trade-off mainly occurs between speed and dissipation. Due to the low specificity in activation and transfer,¹⁹ the change in error due to the variation of these parameters (Figure 2a,c) is actually marginal, especially compared to its variation when the downstream quality control steps are varied (Figure 3b,d). Nevertheless, the two

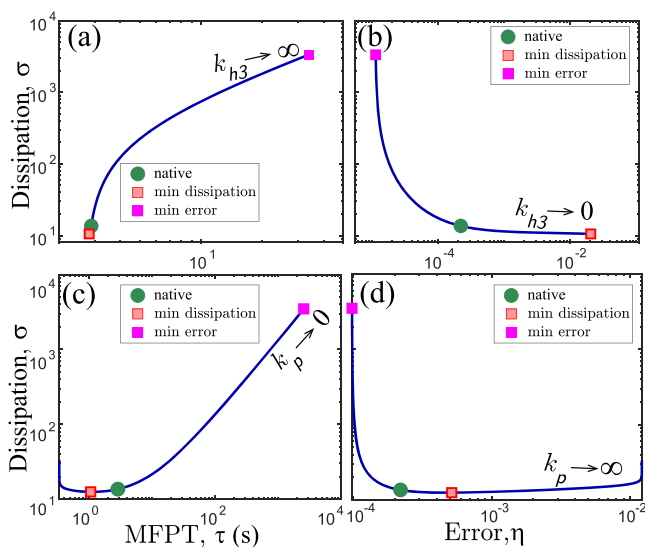


Figure 3. Trade-off among MFPT (τ), error (η), and dissipation (σ) due to variation of the two key quality control processes: the translocation and deacylation of aa-tRNA (k_{h3} , top panels) and product release (k_p , bottom panels). Catalytic rates for the noncognate substrates (k_{h3}' and k_p') are varied proportionally to keep discrimination factors fixed. The green dot denotes the native system. The pink and magenta squares correspond to the positions of the minimum dissipation and error, respectively. When $k_p \rightarrow 0$ or $k_{h3} \rightarrow \infty$, both the MFPT and dissipation diverge to infinity, while the error rate converges to a constant.

reactions take strikingly different strategies in dealing with the trade-off. The activation step prefers to optimize the speed, while the transfer step is near minimal dissipation. The activation step is not rate-limiting; i.e., the maximal speed achieved at $k_a \rightarrow \infty$ is only 4% larger than the native value. However, such an increase in speed leads to a drastic (70%) decrease in dissipation, which is evident from a nearly vertical slope of the curve connecting the green dot and magenta square in Figure 2b. On the other hand, further decreasing the rate of this step would make it rate-limiting as reducing the dissipation by 41% will increase the MFPT by 18-fold. We

hypothesize that the evolution tunes the activation reaction to be on the cusp of being rate-limiting, i.e., to decrease dissipation while keeping the impact on the speed marginal.

In stark contrast, the transfer step rate k_4 is nearly optimized for minimal dissipation; the green dot in Figure 2d is only 0.5% above the minimal value denoted by the pink square. An increase in the transfer rate can reduce the MFPT by 45%, but this will lead to a 50% increase in dissipation. Thus, the increase of MFPT due to optimizing the dissipation in the transfer step is considerably smaller compared to the 18-fold MFPT increase in the activation step (Figure 2b). This finding makes optimization of dissipation in the transfer step more plausible.

Altogether, the results on Figure 2 demonstrate distinct evolutionary optimization strategies in two catalytic steps. IleRS tunes up the amino acid activation rate to guarantee the fast production of aa-tRNA and keeps the transfer rate at an intermediate level so that the dissipation is nearly minimal. These strategies employed enable partial reconciliation of the speed–dissipation trade-off for the enzyme and allow for faster and more efficient formation of aa-tRNA.

Next, we focus on the optimization strategies in key quality control steps. The ability of IleRS to preferentially hydrolyze misacylated products is largely determined by the rate constants for post-transfer editing (k_{h3}) and product release (k_p). The two pre-transfer editing steps exhibit behaviors similar to those of post-transfer editing, but they are less effective in the ability to suppress the error.²⁰ Following the same methodology, we present the results in Figure 3. In contrast to those of activation and transfer, the native rates of the quality control steps reside on a non-trade-off branch of the speed–dissipation curve. For these steps, it is the error that prevents the co-optimization of speed and dissipation. Indeed, improving the accuracy requires either decreasing k_p or increasing k_{h3} and, hence, increasing the proofreading fluxes. Consequently, more ATP is consumed without forming aa-tRNA, and more time will be needed to successfully form a product.

We further explore how the system balances the need for higher accuracy and the resultant cost in terms of slower speed and higher dissipation by examining the position of the native system on the trade-off plots. We find that, in both cases, the native system resides not far from the minimum dissipation/minimum MFPT point. For example, the MFPT of the native system is only 2% above the minimum due to the variation of k_{h3} , and the dissipation in the k_p trade-off plot is only 9% above the minimum value. Although it is hard to claim that either speed or dissipation is the “deal breaker” that makes further improvement in the accuracy unfavorable in evolution, it seems that their combined effect results in a compound cost that decreases the organism’s overall fitness. Consequently, both k_{h3} and k_p are tuned in a way that the MFPT and dissipation are optimized as much as possible as long as the error rate is within a reasonable range, i.e., $\sim 10^{-4}$. Indeed, the fidelity of the aminoacylation needs to surpass only the overall accuracy of protein synthesis ($\eta = 10^{-3}$ to 10^{-4}).^{3–5} Further improvements beyond this threshold will not significantly suppress the protein synthesis error because more mistakes will be made during aa-tRNA selection at the ribosome. Moreover, the accuracy can be further improved through downstream error-correcting mechanisms such as EF-Tu specificity. The need to synthesize numerous proteins continuously raises the necessity of decreasing the cost of time and energy to deliver a single

amino acid while keeping the error rate tolerable. Collectively, these factors rationalize our finding that the proofreading mechanism in *E. coli* IleRS has evolved to adopt an “economic” error-correcting strategy that establishes a reasonable level of fidelity in a speedy and inexpensive fashion.

Our analysis of individual reactions has shown that although different steps can adopt different optimization strategies, most reaction steps optimize IleRS toward an energetic efficiency (i.e., minimal dissipation). However, both our data and previous estimations in the literature suggest that >10% of the ATP hydrolyzed leads to proofreading fluxes, which do not form any products.³⁹ It is therefore unclear whether these futile fluxes are inevitable and whether the local optimization strategies collectively result in the global optimization of dissipation. To address this question, we perform global parameter sampling. To this end, all of the kinetic parameters are varied under the constraints of fixed discrimination factors and fixed chemical potential differences for both futile and product formation cycles (i.e., $\Delta\mu_{\text{ATP}}$ and $\Delta\mu_{\text{p}}$, respectively). The sampling can be regarded as a generalization of the local trade-off analysis. As shown in Figure 4, we found that all

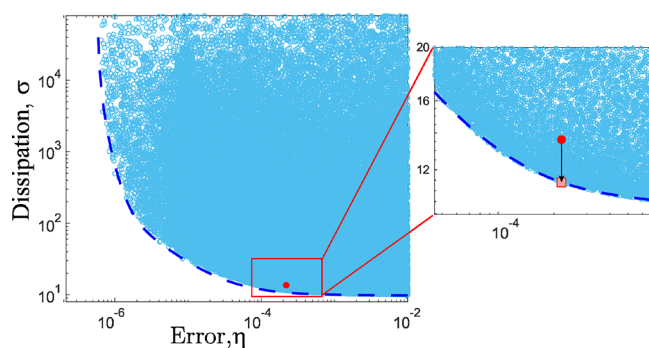


Figure 4. Scatter plot of the error–dissipation relation resulting from the variation of all rate constants. The area to the left or under the blue dashed boundary is inaccessible under any combinations of the rate constants. The red dot indicates the native system; the pink square marks the theoretical minimum dissipation for the native accuracy.

sampled systems always reside on one side of a boundary (blue dashed line) on the error–dissipation plane. Thus, this boundary is a fundamental constraint imposed by the discrimination factors that cannot be circumvented through any variation of the kinetic parameters. The minimum amount of dissipation for any level of accuracy is $\Delta\mu_{\text{p}} = 9.8 k_{\text{B}}T$, which corresponds to the absence of any proofreading. Toward the other end of the spectrum, the error rate can be suppressed as low as $\eta_{\text{min}} \sim 6 \times 10^{-7}$, but the dissipation increases as the error rate decreases and diverges to infinity as the error approaches its minimum. Our results reaffirm the notion that an increased amount of free energy must be dissipated to enhance biological fidelity.^{6,15} On the other hand, the sampling does not put any constraint on the optimal speed, because the time scale of the system can be tuned arbitrarily by varying all of the rate constants proportionally. In reality, however, the kinetic rates are limited by the underlying biochemical processes. For instance, it is hard to conceptualize how the binding rates of ATP and an amino acid to IleRS can exceed the diffusion limit.⁴⁰ These biochemical constraints could reduce the parameter space that can be reached for the actual

system, resulting in a suboptimal performance compared to the theoretical bound discussed here.

The existence of a global lower bound on dissipation for any given error underscores the nonequilibrium nature of biological information processing. In this system, active proofreading resets the system into the initial state without forming a product and, therefore, results in futile ATP hydrolysis. Such proofreading fluxes can improve the system’s accuracy only if the futile cycles are powered by free energy released from ATP hydrolysis. Thus, an increase in proofreading frequency inevitably leads to an increase in dissipation. This trade-off is evidenced by the global dissipation bound that decreases with error (see Figure 4). A similar dissipation–accuracy relation was also found in a system for sensory adaptation, where the optimal dissipation increases with adaptation accuracy and eventually diverges at perfect adaptation, a behavior similar to that of the bound found here.⁴¹ In both cases, dissipation is associated with cyclic futile fluxes that consume free energy to drive the system away from thermodynamic equilibrium. In contrast, the proofreading fluxes in an equilibrium proofreading system (i.e., without any free energy yield from ATP hydrolysis) will not reduce the error of the system.

A detailed inspection of the bottom right area of Figure 4 reveals that the native system resides in the proximity of the error–dissipation boundary. Indeed, the dissipation can at most be decreased by only 16% ($\sim 2.2 k_{\text{B}}T$) without any reduction in accuracy (i.e., from the red dot to the pink square in the inset of Figure 4). As compared to the complete dynamic range of error and dissipation, this is a very small margin. According to the error–dissipation bound, the dissipation must be increased by 3-fold (to $34 k_{\text{B}}T$) to reduce the error rate by 1 order of magnitude (from 10^{-4} to 10^{-5}). This increase is a tremendous cost considering the amount of the amino acid (in this case, isoleucine) required for protein synthesis in the *E. coli* cell cycle. It is therefore understandable that the synthetase has chosen an economic strategy in quality control, as seen in the trade-off analysis of k_{h3} and k_{p} , instead of promoting its accuracy to an unnecessary level.

To understand the evolutionary necessity of multistage proofreading in *E. coli* IleRS, we use our model to assess the importance of different proofreading mechanisms. As shown in Figure 5a, removing both pre-transfer editing pathways causes a marginal increase in error (5%, from purple bars to yellow bars), while removing the post-transfer editing pathway increases the error drastically (by 2 orders of magnitude). This result is consistent with experimental findings that post-transfer editing contributes to the majority of the editing in *E. coli* IleRS.⁵ The pre-transfer proofreading fluxes take up only 12% of all editing fluxes. Notably, this estimate is smaller than the value of 30% derived from a previous kinetic experiment that employed the Michaelis–Menten equation to fit the AMP formation rate.²⁰ This discrepancy is likely because our framework takes into account a more realistic mechanism of the reaction (as compared to the Michaelis–Menten equation).

Given the importance of post-transfer editing, it is intriguing to explore the specific need that caused the evolution of this mechanism. To investigate this, we perform global parameter sampling in the absence of post-transfer editing ($k_{\text{h3}} = k_{\text{h3}'} = 0$) and superimpose the error–dissipation relation onto the native one (see Figure 5b). The addition of post-transfer editing significantly expands the reachable area on the error–dissipation plane. It not only allows IleRS to achieve a higher

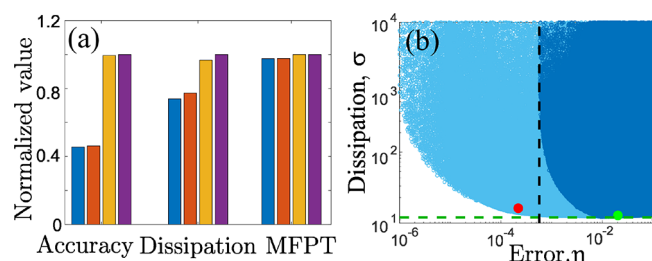


Figure 5. Quantitative comparison of the importance of different proofreading pathways. (a) Key properties for four variants of IleRS: blue, no proofreading; orange, pre-transfer editing only; yellow, post-transfer editing only; purple, native system. The accuracy is defined as $-\ln \eta$. All values are normalized by taking the ratio against the native system. (b) Error–dissipation scatter plot due to global parameter variation: dark blue, samples without post-transfer editing; light blue, samples with a wild type network; red dot, native system ($\eta_{\text{nat}} = 2.2 \times 10^{-4}$); green dot, mutant with only pre-transfer editing ($\eta_{\text{natp}} = 2.0 \times 10^{-2}$). The black dashed line indicates the minimum error for the system without post-transfer editing ($\eta_{\text{min}} = 5.5 \times 10^{-4}$). The green dashed line stands for the minimum dissipation ($\sigma_{\text{min}} = \mu_p = 9.8 k_B T$).

accuracy but also makes it energetically more efficient to maintain an accuracy level that can be attained by pre-transfer editing alone. For each of the optimized systems on the boundary of the dark blue area, there is a system in the light blue area that can achieve the same accuracy with a much lower dissipation. Somewhat surprisingly, the results indicate that even without post-transfer editing, the minimal error [$\eta_{\text{min}} = 5.5 \times 10^{-4}$ (black dashed line in Figure 5b)] is just ~ 2.5 -fold higher than in the native system [$\eta_{\text{nat}} = 2.2 \times 10^{-4}$ (red dot in Figure 5b)]. As discussed above, this level of accuracy could be sufficient. However, the amount of dissipation corresponding to this error rate is astronomical. For example, to reach an error rate that is 3-fold higher than that of the native system ($3\eta_{\text{nat}} = 6.6 \times 10^{-4}$), the dissipation must be increased to at least $200 k_B T$. A further decrease in error requires more and eventually an infinite amount of dissipation as shown by the asymptotic behavior of the boundary of the dark blue area.

Therefore, our results here provide a quantitative rationalization of the evolutionary origin of the IleRS CP1 editing domain. The low discrimination factor in pre-transfer editing (f_{h1} and f_{h2}) makes it energetically costly to maintain a higher accuracy as shown by the accessible region (dark blue area) in Figure 5b. Because both amino acid activation and pre-transfer editing take place within the active site, it might be improbable to improve the pre-transfer editing specificity any further without affecting the transfer efficacy. Consequently, a separate domain is recruited for post-transfer editing, which provides a more economic way of maintaining genetic code fidelity. The existence of multiple proofreading pathways successfully improves the overall fitness by relaxing the trade-off between error and dissipation. Consistent with this prediction, a high degree of conservation in CP1 domains for IleRS, ValRS, and LeuRS proteins suggests early emergence and selective pressure to maintain post-transfer editing.⁴²

In summary, our biophysical model with parameters derived from experiments leads to valuable insights into the interplay among speed, accuracy, and dissipation for the isoleucyl-tRNA synthetase. As a prerequisite to peptide synthesis at the ribosome, it is essential to maintain a high speed and energetic efficiency of aa-tRNA synthesis. However, we discovered that their co-optimization is prevented by a dissipation–speed

trade-off in key catalytic steps. Generalizing the previous viewpoint on the existence of a universal preference to improving some properties at the cost of the others,¹⁶ we provide a new perspective that different priorities of individual reaction steps enable partial reconciliation of the trade-offs.

Despite its potential to reduce the error significantly [by 2 orders of magnitude (see Figure 4)], it seems that the IleRS has adopted an “economic” strategy that improves speed and dissipation as much as possible and maintains the error at a reasonable level. We demonstrate the extent to which dissipation is optimized by the proximity of the native system to a fundamental error–dissipation bound. The results are further rationalized by several biological arguments, including the error threshold imposed by the downstream aa-tRNA selection ($\eta = 10^{-3}$ to 10^{-4}) and the demand for rapid and energetically inexpensive aa-tRNA supply for protein synthesis. Once the accuracy of aaRS surpassed that of aa-tRNA selection, evolutionary forces no longer drove any enhancement of accuracy. Instead, reducing MFPT and dissipation became the priorities for IleRS. This hypothesis could be experimentally tested by investigating whether the dissipation can be reduced in IleRS mutants without impairing the overall fidelity of protein translation.

Our results not only provide a new understanding of the aminoacylation process but also construct a general framework for analyzing complicated discriminatory proofreading networks. We argue that the importance of one reaction pathway can never be fully appreciated by looking at one property in isolation. Instead, one should examine the accessible region in the space spanned by the characteristic properties such as the error–dissipation plane studied here. From this perspective, the significance of post-transfer editing lies not in reducing the minimum error rate but in making it less energetically costly to maintain an error rate of $\eta \sim 10^{-4}$. The existence of a dissipation–error lower bound (blue dashed line, Figure 4) indicates a minimum cost for biological error correction that is imposed by the discrimination factors. Further studies of this minimum energy cost may provide new insights into the underlying thermodynamic principle of biological information processing.

■ ASSOCIATED CONTENT

Supporting Information

The Supporting Information is available free of charge at <https://pubs.acs.org/doi/10.1021/acs.jpcllett.0c01073>.

Detailed description of the tRNA^{Ile} aminoacylation model (including the methods for estimation of the kinetic parameters) and mathematical formalism and definitions of error rate η , MFPT τ , and energy dissipation σ (PDF)

■ AUTHOR INFORMATION

Corresponding Author

Oleg A. Igoshin – Department of Bioengineering, Department of Chemistry, Department of Biosciences, and Center for Theoretical Biological Physics, Rice University, Houston, Texas 77005, United States; orcid.org/0000-0002-1449-4772; Email: igoshin@rice.edu

Authors

Qiwei Yu – School of Physics, Peking University, Beijing 100871, China; Center for Theoretical Biological Physics, Rice University, Houston, Texas 77005, United States

Joel D. Mallory – Center for Theoretical Biological Physics, Rice University, Houston, Texas 77005, United States; orcid.org/0000-0002-0251-5724

Anatoly B. Kolomeisky – Center for Theoretical Biological Physics, Department of Chemistry, Department of Chemical and Biomolecular Engineering, and Department of Physics and Astronomy, Rice University, Houston, Texas 77005, United States; orcid.org/0000-0001-5677-6690

Jiqiang Ling – Department of Cell Biology and Molecular Genetics, The University of Maryland, College Park, Maryland 20742, United States; orcid.org/0000-0003-4466-8304

Complete contact information is available at:

<https://pubs.acs.org/10.1021/acs.jpcllett.0c01073>

Notes

The authors declare no competing financial interest.

ACKNOWLEDGMENTS

This work was supported by Welch Foundation Grant C-1995 to O.A.I. and Center for Theoretical Biological Physics National Science Foundation (NSF) Grant PHY-1427654. A.B.K. also acknowledges support from Welch Foundation Grant C-1559. J.L. acknowledges support from NINDS grant R21NS101245. Q.Y. acknowledges support from the Chinese Scholarship Council (CSC).

REFERENCES

- (1) Kunkel, T. A.; Bebenek, K. DNA replication fidelity. *Annu. Rev. Biochem.* **2000**, *69*, 497–529.
- (2) Watson, J. D.; Baker, T. A.; Bell, S. P.; Gann, A. A. F.; Levine, M.; Losick, R. M. *Molecular biology of the gene*, 6th ed.; Pearson/Benjamin Cummings, 2007.
- (3) Reynolds, N. M.; Lazazzera, B. A.; Ibba, M. Cellular mechanisms that control mistranslation. *Nat. Rev. Microbiol.* **2010**, *8*, 849–856.
- (4) Zaher, H. S.; Green, R. Fidelity at the molecular level: lessons from protein synthesis. *Cell* **2009**, *136*, 746–762.
- (5) Cvetic, N.; Bilus, M.; Gruic-Sovulj, I. The tRNA A76 hydroxyl groups control partitioning of the tRNA-dependent pre- and post-transfer editing pathways in class I tRNA synthetase. *J. Biol. Chem.* **2015**, *290*, 13981–13991.
- (6) Hopfield, J. J. Kinetic proofreading: A new mechanism for reducing errors in biosynthetic processes requiring high specificity. *Proc. Natl. Acad. Sci. U. S. A.* **1974**, *71*, 4135–4139.
- (7) Ninio, J. Kinetic amplification of enzyme discrimination. *Biochimie* **1975**, *57*, 587–595.
- (8) Nangle, L. A.; de Crécy Lagard, V.; Döring, V.; Schimmel, P. Genetic code ambiguity. *J. Biol. Chem.* **2002**, *277*, 45729–45733.
- (9) Schimmel, P. Development of tRNA synthetases and connection to genetic code and disease. *Protein Sci.* **2008**, *17*, 1643–1652.
- (10) Murugan, A.; Huse, D. A.; Leibler, S. Speed, dissipation, and error in kinetic proofreading. *Proc. Natl. Acad. Sci. U. S. A.* **2012**, *109*, 12034–12039.
- (11) Sartori, P.; Pigolotti, S. Kinetic versus energetic discrimination in biological copying. *Phys. Rev. Lett.* **2013**, *110*, 188101.
- (12) Murugan, A.; Huse, D. A.; Leibler, S. Discriminatory proofreading regimes in nonequilibrium systems. *Phys. Rev. X* **2014**, *4*, 021016.
- (13) Sartori, P.; Pigolotti, S. Thermodynamics of error correction. *Phys. Rev. X* **2015**, *5*, 041039.
- (14) Banerjee, K.; Kolomeisky, A. B.; Igoshin, O. A. Elucidating interplay of speed and accuracy in biological error correction. *Proc. Natl. Acad. Sci. U. S. A.* **2017**, *114*, 5183–5188.
- (15) Wong, F.; Amir, A.; Gunawardena, J. Energy-speed-accuracy relation in complex networks for biological discrimination. *Phys. Rev. E: Stat. Phys., Plasmas, Fluids, Relat. Interdiscip. Top.* **2018**, *98*, 012420.
- (16) Mallory, J. D.; Kolomeisky, A. B.; Igoshin, O. A. Trade-offs between error, speed, noise, and energy dissipation in biological processes with proofreading. *J. Phys. Chem. B* **2019**, *123*, 4718–4725.
- (17) Johnson, K. A. Conformational coupling in DNA polymerase fidelity. *Annu. Rev. Biochem.* **1993**, *62*, 685–713.
- (18) Gromadski, K. B.; Rodnina, M. V. Kinetic determinants of high-fidelity tRNA discrimination on the ribosome. *Mol. Cell* **2004**, *13*, 191–200.
- (19) Dulic, M.; Cvetic, N.; Perona, J. J.; Gruic-Sovulj, I. Partitioning of tRNA-dependent editing between pre- and post-transfer pathways in class I aminoacyl-tRNA synthetases. *J. Biol. Chem.* **2010**, *285*, 23799–23809.
- (20) Dulic, M.; Perona, J. J.; Gruic-Sovulj, I. Determinants for tRNA-dependent pretransfer editing in the synthetic site of isoleucyl-tRNA synthetase. *Biochemistry* **2014**, *53*, 6189–6198.
- (21) Ling, J.; Reynolds, N.; Ibba, M. Aminoacyl-tRNA synthesis and translational quality control. *Annu. Rev. Microbiol.* **2009**, *63*, 61–78.
- (22) Bacher, J. M.; Schimmel, P. An editing-defective aminoacyl-tRNA synthetase is mutagenic in aging bacteria via the SOS response. *Proc. Natl. Acad. Sci. U. S. A.* **2007**, *104*, 1907–1912.
- (23) Nureki, O.; Vassilyev, D. G.; Tateno, M.; Shimada, A.; Nakama, T.; Fukai, S.; Konno, M.; Hendrickson, T. L.; Schimmel, P.; Yokoyama, S. Enzyme structure with two catalytic sites for double-sieve selection of substrate. *Science* **1998**, *280*, 578–582.
- (24) Freist, W. Isoleucyl-tRNA synthetase: An enzyme with several catalytic cycles displaying variation in specificity and energy consumption. *Angew. Chem., Int. Ed. Engl.* **1988**, *27*, 773–788.
- (25) Fersht, A. R. Editing mechanisms in protein synthesis. Rejection of valine by the isoleucyl-tRNA synthetase. *Biochemistry* **1977**, *16*, 1025–1030.
- (26) Bennett, B. D.; Kimball, E. H.; Gao, M.; Osterhout, R.; Van Dien, S. J.; Rabinowitz, J. D. Absolute metabolite concentrations and implied enzyme active site occupancy in *Escherichia coli*. *Nat. Chem. Biol.* **2009**, *5*, 593–599.
- (27) Neidhardt, F. C.; Ingraham, J. L.; Schaechter, M. *Physiology of the bacterial cell: A molecular approach*; Sinauer Associates, 1990.
- (28) Dong, H.; Nilsson, L.; Kurland, C. G. Co-variation of tRNA abundance and codon usage in *Escherichia coli* at different growth rates. *J. Mol. Biol.* **1996**, *260*, 649–663.
- (29) Dittmar, K. A.; Sorensen, M. A.; Elf, J.; Ehrenberg, M.; Pan, T. Selective charging of tRNA isoacceptors induced by amino-acid starvation. *EMBO Rep.* **2005**, *6*, 151–157.
- (30) Kukko-Kalske, E.; Lintunen, M.; Inen, M. K.; Lahti, R.; Heinonen, J. Intracellular PPi concentration is not directly dependent on amount of inorganic pyrophosphatase in *Escherichia coli* K-12 cells. *J. Bacteriol.* **1989**, *171*, 4498–4500.
- (31) Frey, P. A.; Arabshahi, A. Standard free energy change for the hydrolysis of the α , β -phosphoanhydride bridge in ATP. *Biochemistry* **1995**, *34*, 11307–11310.
- (32) Spirin, A. S. *Ribosomes*; Springer US: Boston, 1999.
- (33) MacDonald, C.; Yu, D.; Buibas, M.; Silva, G. Diffusion modeling of ATP signaling suggests a partially regenerative mechanism underlies astrocyte intercellular calcium waves. *Front. Neuroeng.* **2008**, *1*, 1.
- (34) Azarashvili, T. S.; Odinkova, I. V.; Krestinina, O. V.; Baburina, Y. L.; Grachev, D. E.; Teplova, V. V.; Holmuhamedov, E. L. Role of phosphorylation of porine proteins in regulation of mitochondrial outer membrane under normal conditions and alcohol intoxication. *Biol. Membr.* **2011**, *28*, 14–24.
- (35) Potts, R. O.; Ford, N. C.; Fournier, M. J. Changes in the solution structure of yeast phenylalanine transfer ribonucleic acid associated with aminoacylation and magnesium binding. *Biochemistry* **1981**, *20*, 1653–1659.

- (36) Biro, J. C. The concept of RNA-assisted protein folding: the role of tRNA. *Theor. Biol. Med. Modell.* **2012**, *9*, 10.
- (37) Plochowitz, A.; Farrell, I.; Smilansky, Z.; Cooperman, B. S.; Kapanidis, A. N. In vivo single-RNA tracking shows that most tRNA diffuses freely in live bacteria. *Nucleic Acids Res.* **2017**, *45*, 926–937.
- (38) Hill, T. L. *Free energy transduction in biology*; Academic Press, 1977.
- (39) Freter, R. R.; Savageau, M. A. Proofreading systems of multiple stages for improved accuracy of biological discrimination. *J. Theor. Biol.* **1980**, *85*, 99–123.
- (40) Torney, D. C.; McConnell, H. M. Diffusion-limited reaction rate theory for two-dimensional systems. *Proc. R. Soc. A* **1983**, *387*, 147–170.
- (41) Lan, G.; Sartori, P.; Neumann, S.; Sourjik, V.; Tu, Y. The energy–speed–accuracy trade-off in sensory adaptation. *Nat. Phys.* **2012**, *8*, 422–428.
- (42) Bullwinkle, T. J.; Ibba, M. In *Aminoacyl-tRNA synthetases in biology and medicine*; Kim, S., Ed.; Springer Netherlands: Dordrecht, The Netherlands, 2014; pp 43–87.